Journal of Biomedical Optics

SPIEDigitalLibrary.org/jbo

Identifying compositional and structural changes in spongy and subchondral bone from the hip joints of patients with osteoarthritis using Raman spectroscopy

Tomasz Buchwald
Krzysztof Niciejewski
Marek Kozielski
Mirosław Szybowicz
Marcin Siatkowski
Hanna Krauss

SPIE

Identifying compositional and structural changes in spongy and subchondral bone from the hip joints of patients with osteoarthritis using Raman spectroscopy

Tomasz Buchwald,[a] Krzysztof Niciejewski,[b] Marek Kozielski,[a] Mirosław Szybowicz,[a] Marcin Siatkowski,[c,d] and Hanna Krauss[b]
[a]Poznan University of Technology, Faculty of Technical Physics, Nieszawska 13a, 60-965 Poznań, Poland
[b]Poznan University of Medical Sciences, Faculty of Medicine I, Święcickiego 6, 60-784 Poznań, Poland
[c]DZNE, German Center for Neurodegenerative Disorders, Gehlsheimer Strasse 20, D-18147 Rostock, Germany
[d]University of Rostock, Institute for Biostatistics and Informatics in Medicine and Ageing Research, Ernst Heydemann-Strasse 8, D-18057 Rostock, Germany

Abstract. Raman microspectroscopy was used to examine the biochemical composition and molecular structure of extracellular matrix in spongy and subchondral bone collected from patients with clinical and radiological evidence of idiopathic osteoarthritis of the hip and from patients who underwent a femoral neck fracture, as a result of trauma, without previous clinical and radiological evidence of osteoarthritis. The objectives of the study were to determine the levels of mineralization, carbonate accumulation and collagen quality in bone tissue. The subchondral bone from osteoarthritis patients in comparison with control subject is less mineralized due to a decrease in the hydroxyapatite concentration. However, the extent of carbonate accumulation in the apatite crystal lattice increases, most likely due to deficient mineralization. The alpha helix to random coil band area ratio reveals that collagen matrix in subchondral bone is more ordered in osteoarthritis disease. The hydroxyapatite to collagen, carbonate apatite to hydroxyapatite and alpha helix to random coil band area ratios are not significantly changed in the differently loaded sites of femoral head. The significant differences also are not visible in mineral and organic constituents' content in spongy bone beneath the subchondral bone in osteoarthritis disease. [DOI: 10.1117/1.JBO.17.1.017007]

Keywords: osteoarthritis; subchondral bone; spongy bone; Raman; composition; structure.

Paper 11454 received Aug. 22, 2011; revised manuscript received Nov. 9, 2011; accepted for publication Nov. 30, 2011; published online Jan. 31, 2012.

1 Introduction

Osteoarthritis (OA) is a chronic, slowly progressive, degenerative joint disease, leading to pain and disability. OA is characterized by the degeneration of the articular cartilage and changes in the structure of calcified cartilage and underlying subchondral bone.[1–4] OA is classified as either primary or secondary. Primary OA occurs without an obvious cause or because of the accumulation of mechanical damage. Secondary OA occurs as a response to trauma, previous injury, obesity or metabolic disease.[5,6] In humans, the pathogenesis of OA is exceedingly complex, involving genetic and environmental factors as well as local biomechanical factors. More recent studies have shown that OA affects not only the articular cartilage, but the whole joint, also synovium, synovial fluid, calcified cartilage and subchondral bone.[4,7–9] Some hypotheses about the initiation of OA have been proposed in the past years. One of them considers that bone may be the primary organ triggering OA, and the stiffening of the subchondral bone leads to a decrease in shock absorbency with cartilage damage due to overloading.[10,11] However, previous studies have not confirmed any hypothesis concerning the etiology of OA, and it is still unknown what causes the subchondral bone changes. The role of bone in OA has been examined and indication of OA is thickening and decreased mineralization of the subchondral bone plate and extensive remodeling reaction in the subchondral and spongy bone regions.[12–17] These studies support the idea that OA is a disease that affects the entire joint including the bone tissue.

The hip joint is a complex biological system comprised of hyaline articular cartilage, calcified cartilage, synovial fluid and synovial membrane. Articular cartilage is non-mineralized in the surface layers but contains a layer of mineralized tissue adjacent to subchondral bone that is built with cortical bone.[18–20] The bone that directly lies under subchondral bone is spongy bone, also known as trabecular or cancellous bone. The bone is a unique type of connective tissue composed of certain types of cells, such as osteoblasts, osteocytes, osteoclasts, and extracellular matrix, which consists of an organic matrix and mineral components (hydroxyapatite and carbonate apatite crystals).[21,22] The organic matrix is made in 90% by type I collagen fibers.[23] The collagen secondary structure is referred to an alpha helix (α-helix) and beta sheet (β-sheet). Alpha helix is a basic structure of organic matrix in bone tissue. The collagen that is neither alpha helix nor beta sheet has been referred to as a random coil. This disordered structure does not conform to any frequently recurring pattern.[24–26]

In the earlier studies, spectroscopic methods including infrared and Raman spectroscopy have been used to study cartilage and bone tissue.[27–34] The published results have shown high

Address all correspondence to: Tomasz Buchwald, Poznan University of Technology, Faculty of Technical Physics, Nieszawska 13a, 60-965 Poznań, Poland. Fax: +48616653200; E-mail: tomasz.buchwald@poczta.onet.pl.

0091-3286/2012/$25.00 © 2012 SPIE

potential in distinguishing normal and abnormal characteristics of the sample. The use of vibrational spectroscopies in biological investigation offers several advantages. First, these physical techniques give information about the structure and composition of studied material at the molecular level. Second, spectroscopic data are obtained in a noninvasive manner or minimally invasive method, so the same sample can be examined by various analytical methods. Third, there is no limit to the size, allowing a study of a large area of a sample.[35] Properties of Raman spectroscopy (micro-Raman spectroscopy) method that make it more attractive than infrared spectroscopy method for direct analysis of biological tissues, include high spatial resolution (0.5 to 1 μm) and limited spectral interference from water. The visible or near-infrared optics that are used by Raman instruments are compatible with fiberoptic probes used in clinical instruments such as arthroscopes. In this way, Raman spectroscopy could be used directly in arthroscopic surgery. Esmonde-White et al. showed the use of Raman spectroscopy for arthroscopy of human joint tissues using a custom-built fiberoptic probe.[36] Raman and infrared spectroscopy methods are especially useful to distinguish normal and pathological tissue and understand disease progression. In particular, Raman and infrared spectroscopy methods can provide detailed chemical information on the mineral and collagen matrix components of bone tissue. Recently, the capabilities of these techniques have been used to examine synovial fluid, articular cartilage, subchondral bone and spongy bone from the animals and humans with OA.[37–44] Although osteoarthritic subchondral and spongy bone were often investigated, very little is known about the composition and structure of this mineralized tissue beneath the articular cartilage.

Examination of compositional and structural properties of spongy and subchondral bone and better understanding the role of bone in disease progression is very important in analyzing the etiology of OA and assessing treatment in patients. The difficulties in clinical diagnosis of OA are essentially due to the complexity of this disease. Most cases of OA are unfortunately only identified in the advanced stages. Identification of OA in its early stages is critical to disease management. Raman spectroscopy may help with early diagnosis of OA by providing insight into the composition and structure of joint degeneration. The goal of this work was to examine the chemical composition and molecular structure of extracellular matrix in spongy and subchondral bone from the femur heads of patients with OA of the hip joint using the Raman spectroscopy method. The material properties of spongy and subchondral bone from patients with OA were compared with a control group. In particular, the objectives of the study were to determine the levels of mineralization (hydroxyapatite/collagen ratio), carbonate accumulation (carbonate apatite/hydroxyapatite ratio) and collagen quality (alpha helix/random coil ratio). The hydroxyapatite to collagen band area ratio provides an indication of bone mineralization and the carbonate apatite to hydroxyapatite band area ratio was used to describe the degree of carbonate substitution in the apatite crystal lattice. The collagen quality parameter indicate the alpha helix content in collagen's secondary structure and the degree of distortion of collagen crosslinks in bone matrix.

2 Materials and Methods

In this study, Raman spectroscopy was used to estimate the biochemical composition and structure of spongy and subchondral bone of femoral heads collected from 10 patients with clinical and radiological evidence of idiopathic OA of the hip and from 10 patients who underwent a femoral neck fracture, as a result of trauma, without previous clinical and radiological evidence of OA. These fractures were not related to any metabolic bone disease. The group of patients without bone disease were defined as the control group. Dooley et al.[45] reported that the external stress occurs at sites of bone distant from fractures. In this study, the samples were selected from sites of femoral head, where the external stress connected with bone fracture do not influence spectral parameters of Raman bands. The study population consisted of OA group of seven women and three men between 49 and 88 years of age and control group of five women and five men between 50 and 77 years of age. The average age for OA and control patients was 71.9 and 63, respectively. The treatment of choice in the above mentioned patients was hip replacement surgery (total hip arthroplasty). The cross-sections of 5 mm in thickness were obtained from heads of femurs. In this way, subchondral and underlying spongy bone were analyzed without removal of cartilage. The samples were cut from three defined sites of these cross-sections in each femur head. These three sites were subjected to different loads in vivo: from the central site of femoral head to analyze spongy bone, from superolateral and inferomedial sites of femoral head to analyze subchondral bone and underlying spongy bone (Fig. 1). The superolateral and inferomedial regions are the most and the least weight-bearing surface of femoral head, respectively (Fig. 1, adapted from Batra and Charnley).[46] Clinical assessment of OA was made from a combination of x-ray and patient history for OA symptoms. In this work, overall severity of OA was graded using Kellgren and Lawrence grading scale (the grading system of x-ray features) defined as follows: 0 = normal, no OA, 1 = doubtful OA, 2 = minimal OA, 3 = moderate OA, and 4 = severe OA.[47,48] Patients with Kellgren and Lawrence grades 0–1 were considered negative for radiological evidence of OA. Patients with Kellgren and

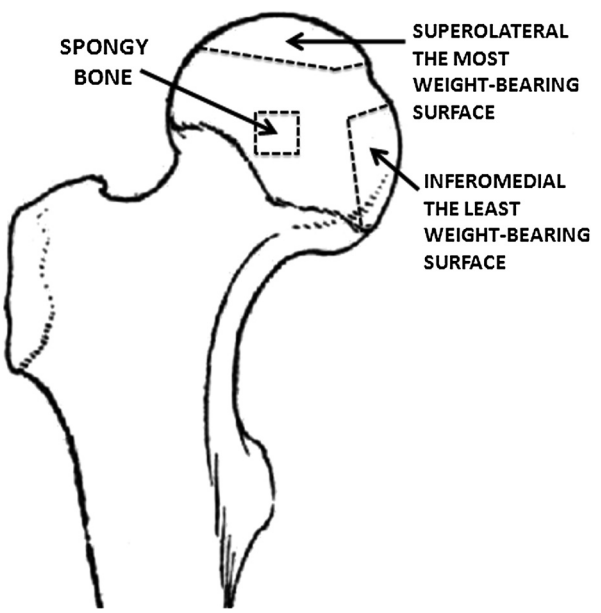

Fig. 1 Schematic diagram of the human femoral head with sites from which samples of spongy and subchondral bone were selected.

Lawrence grades 2 to 4 were considered positive for radiological evidence of OA. Figure 2 displays x-ray images of two hip joints with different Kellgren and Lawrence grades: grade 1—the hip joint on the left; grade 3—the hip joint on the right. The average Kellgren and Lawrence value for OA and control patients were 3.3 and 0.4, respectively. The study has received the approval of the local Bioethical Commission at the Poznan University of Medical Sciences (No 843/09 from 8 October 2009).

All the measurements were carried out on inVia Renishaw micro-Raman system with diode-pumped laser, emitting 785 nm near-infrared wavelength. The Raman scattering spectra of bone tissue were recorded in the back scattering geometry in non-confocal mode in the spectral range of 200 to 3200 cm^{-1}. The laser beam was tightly focused on the sample surface through a Leica 50× LWD microscope objective (LWD—long working distance) with numerical aperture (NA) equal to 0.5 leading to a laser beam diameter about 2 μm. During measurements, to prevent any damages of the sample, an excitation power was fixed at 5 mW. The position of the microscope objective with respect to the bone tissue was piezoelectrically controlled in the three axes during surface mapping. The Raman images of surface of subchondral and spongy bone were acquired in rectangular areas of 50×50 μm^2 and at 10 μm step size. Seven Raman maps were measured in each defined site (the central site of femur head to analyze spongy bone, superolateral and inferomedial sites of femur head to analyze subchondral bone and underlying spongy bone). Single spectrum was obtained as the sum of spectra in each map, then this single spectrum was analyzed. In this way, seven single spectrum of each defined site allowed us to obtain average value of compositional and structural parameters of each femur head. The time of exposure to get individual Raman spectra was 10 s, the spectra were recorded without accumulation. The incident light was linearly polarized and Raman scattered light was detected without polarizing optics. The samples were measured in room temperature. Raman bands were fitted to Lorentzian/Gaussian peaks. Cosmic ray artifacts were removed and band spectral parameters were obtained by deconvolution in the WIRE 3.1 (Renishaw) software. The deconvolution was used in each interesting region of spectrum of bone tissue.

Assumption of groups normality distribution origin were tested by Lilliefors normality test (P-values > 0.05) and were followed by variance homogeneity Bartlett tests (P-values > 0.05). To determine whether the differently loaded sites of femoral head and osteoarthritis have an effect on spongy and subchondral bone composition and structure, we have conducted 2-way ANOVA. No significance of factors and interaction were found in spongy bone, in contrast to subchondral bone. Thus, post-hoc Tukey's HSD procedure was applied to subchondral bone compositional and structural parameters with 95% family-wise confidence level. All statistical analyses were performed using R statistical computing and graphics environment.[49]

3 Results and Discussion

Figure 3 shows a typical Raman spectrum of bone tissue. The major bands in Raman spectra of bone tissue corresponding to mineral and organic phases are labeled. The bands assigned to organic components (collagen and non-collagen moieties) are found in region: ∼1200 to 1320 cm^{-1} (amide III), ∼1595 to 1700 cm^{-1} (amide I), ∼1400 to 1470 cm^{-1} and ∼2800 to 3100 cm^{-1} (bending and stretching modes of C-H groups).[33,50] The phosphate group (PO_4^{3-}) associated with mineral components has four internal vibration modes: ν_1 (∼960 to 961 cm^{-1}), ν_2 (∼430 to 450 cm^{-1}), ν_3 (∼1035 to 1048 cm^{-1} and ∼1070 to 1075 cm^{-1}), ν_4 (∼587 to 604 cm^{-1}).[33,51,52] The internal modes of the carbonate group (CO_3^{2-}) are detected at 1073 cm^{-1} (ν_1 mode of B-type carbonate) and 1103 cm^{-1} (mode of A-type carbonate).[33] However, the weakness of the A-type carbonate band does not permit getting information about the composition of bone tissue; thus, only B-type mode is used. The Raman signal depends not only on the composition but also on the local orientation of collagen fibers or apatite crystals. However, multiple scattering in turbid bone tissue cause light depolarization. The use of the smallest depth of field allows minimization of depolarization effects.[53] In this work, Raman spectra of bone tissue were recorded in non-confocal mode; therefore, bands in Raman spectrum of bone tissue were not sensitive to orientation effect.

Area integrations were performed to determine hydroxyapatite to collagen ratios (phosphate 960 cm^{-1}/amide III 1244 cm^{-1} and 1268 cm^{-1}), carbonate apatite to hydroxyapatite

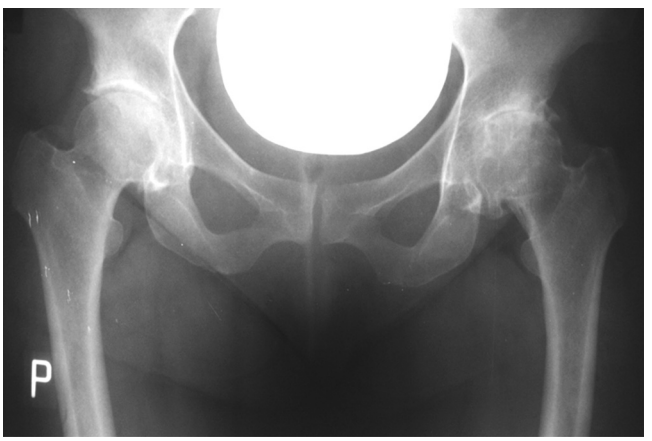

Fig. 2 X-ray image of two hip joints. Kellgren and Lawrence grades: grade 1—the hip joint on the left, grade 3—the hip joint on the right.

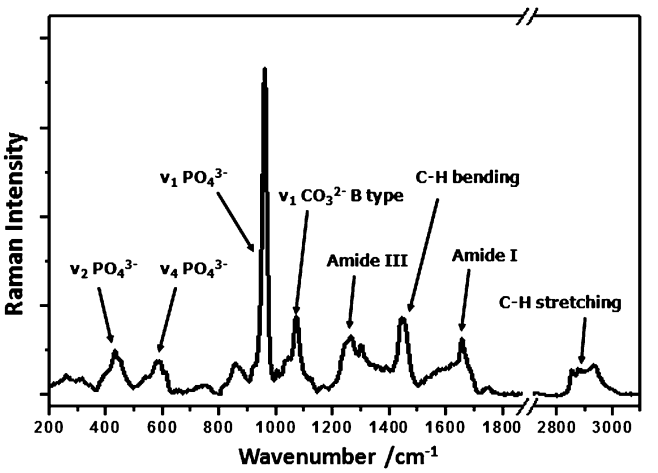

Fig. 3 Typical Raman spectrum of bone tissue showing the major bands and the corresponding compounds. Background signal has been removed.

ratios (carbonate 1071 cm^{-1}/phosphate 960 cm^{-1}) and disorder in collagen's secondary structure via amide III (alpha helix 1268 cm^{-1}/random coil 1244 cm^{-1}). The intensity of individual Raman bands cannot be used as an empirical measure of the mineral and organic components content in bone tissue because the irregularity of biological material surface strongly influences the bands intensity. Due to potential variations in distance from the objective to the sample, the band area ratios were employed. Ratios of these bands gave information on the relation of the mineral and organic components content in the spongy and subchondral bone. The proposed parameters to estimate the chemical composition and structure of bone tissue were used in previous Raman investigations.[41,51,54–56]

The Raman spectra were measured in subchondral and spongy bone of femoral heads collected from two groups: OA patients group and control group. The analysis of Raman spectra of bone tissue determines the degree of bone mineralization, the carbonate accumulation in the apatite crystal lattice, and distortion of collagen cross-links in bone matrix. Figure 4(a) presents the content of hydroxyapatite crystals with respect to that of collagen (the hydroxyapatite to collagen band area ratio) in subchondral bone from the most and the least weight-bearing surface of femoral heads. Raman spectroscopy results showing that subchondral bone from the hip joints of patients with OA is less mineralized. The band area ratio of the hydroxyapatite to collagen in subchondral bone from the hip joints of OA patients and control group are significantly different ($P < 0.0001$). We believe that demineralization of subchondral bone is a result of greater remodeling of OA bone tissue. The level of mineralization in the subchondral bone from the most weight-bearing surface of femoral head is slightly lower compared with the level of mineralization from the least weight-bearing surface for patients with OA and the control group; however, this difference is not statistically significant ($P = 0.7378$ for OA patients and $P = 0.7413$ for control group). There are no significant differences in the content of hydroxyapatite crystals between OA patients and control subject in the underlying spongy bone ($P = 0.5970$). The difference in mineralization in trabeculae, as seen in Fig. 4(b), is not significant in the most weight-bearing surface, the least weight-bearing surface and central site of femoral head ($P = 0.9346$).

Figures 5(a) and 5(b) present the carbonate apatite to hydroxyapatite band area ratio data for OA patients and control subject from subchondral and spongy bone, respectively. The carbonate apatite to hydroxyapatite band area ratio is a spectroscopic parameter that indicates carbonate ion substitution into the apatite mineral. The extent of carbonate accumulation in the apatite crystal lattice is significantly higher ($P < 0.0001$) in the subchondral bone from OA patients than from control group [Fig. 5(a)]. It is possible that the increased carbonate substitution occurred in response to deficient mineralization. Differences in the band area ratio of carbonate apatite to hydroxyapatite in the subchondral bone between the most and the least weight-bearing surface of femoral heads are not significant for OA patients ($P = 0.7037$) and control group ($P = 0.9554$). As seen in Fig. 5(b), no significant differences ($P = 0.1069$) are observed in carbonate apatite to hydroxyapatite band area ratio in the spongy bone tissue from the layer close to the subchondral bone and from the central site of femoral head between OA patients and control group. There are also no significant differences in the carbonate content in the most weight-bearing surface, the least weight-bearing surface and central site of femoral head in spongy bone ($P = 0.9153$).

The collagen quality parameter used in Raman spectroscopy indicates the collagen's secondary structure and the degree of distortion of collagen crosslinks in bone matrix. This parameter could be obtained by deconvolution of amide I or amide III envelopes.[31,57] In this work, the amide III band was only used to assess the ordered secondary structure such as alpha helix and disordered secondary structure such as random coil. Two maxima of the bands were observed within the amide III envelope. The band maximum at 1244 cm^{-1} was assigned to random coil conformation and the band maximum at 1268 cm^{-1} was assigned to alpha helix conformation.[58] The ratio of the 1268 cm^{-1}/1244 cm^{-1} band areas has been used in Raman studies to assess collagen quality.[41] Figures 6(a) and 6(b) present the alpha helix to random coil content for OA patients and control subject from subchondral and spongy bone, respectively. The values of the alpha helix to random coil band area ratio are significantly different ($P < 0.0001$) in subchondral bone from the hip joints of OA patients and control group and reveal that collagen matrix is less ordered in the

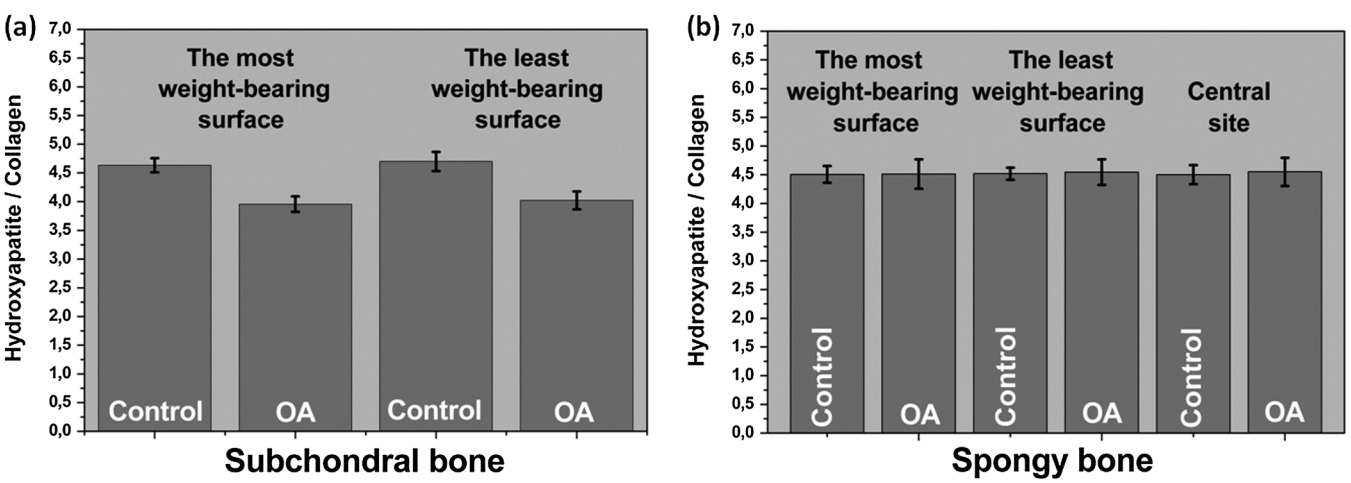

Fig. 4 The ratio of hydroxyapatite to collagen band area in subchondral bone (a) and spongy bone (b) of femoral heads for OA patients and control group.

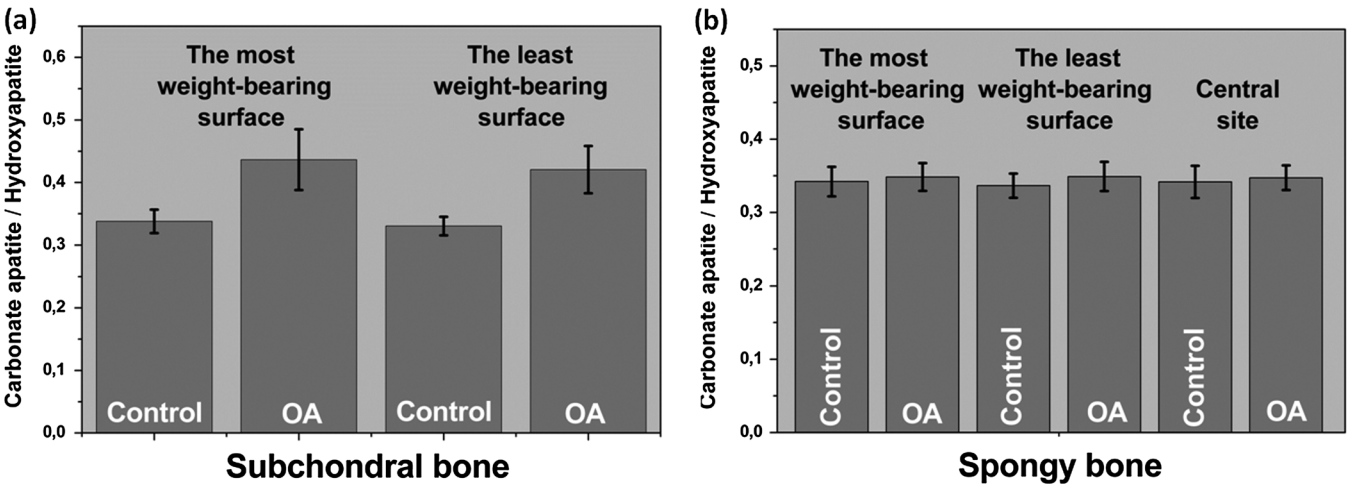

Fig. 5 The ratio of carbonate apatite to hydroxyapatite band area in subchondral bone (a) and spongy bone (b) of femoral heads for OA patients and control group.

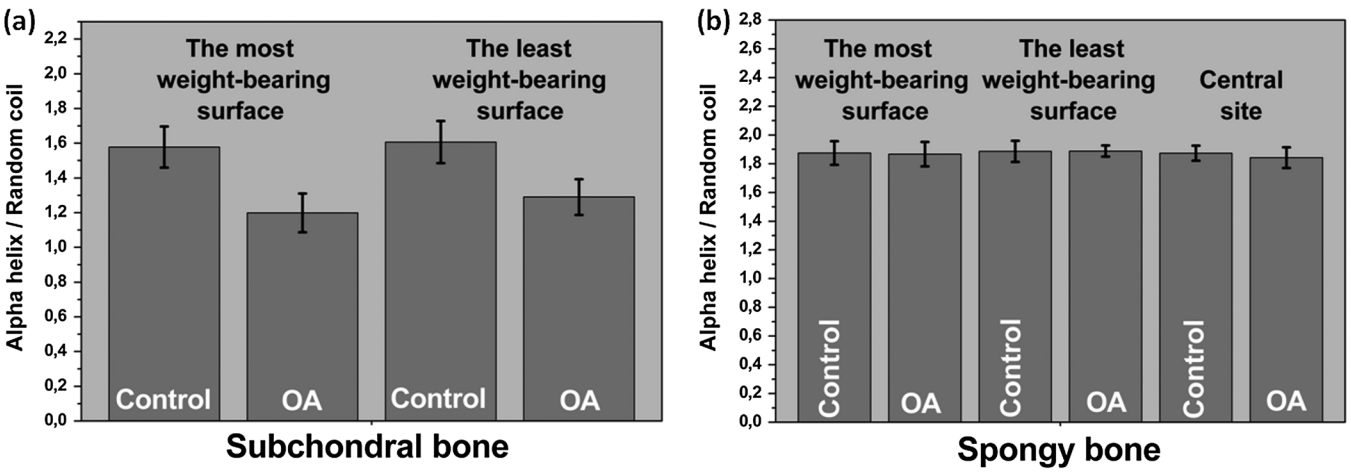

Fig. 6 The ratio of alpha helix to random coil band area in subchondral bone (a) and spongy bone (b) of femoral heads for OA patients and control group.

subchondral bone of OA patients. The degree of alpha helical structure to disordered structure transition increase with OA disease progression. Raman spectra of subchondral bone showed slight increase in the relative abundance of disordered collagen's secondary structure in the most weight-bearing surface of femoral head for OA patients and control group, although the difference was not significant ($P = 0.2887$ for OA patients and $P = 0.9409$ for control group). As seen in Fig. 6(b), no significant differences ($P = 0.4807$) are observed in the alpha helix to random coil band area ratio in the spongy bone tissue from the layer close to the subchondral bone and from the central site of femoral head between the OA patients and control group. Scores from the most weight-bearing surface, the least weight-bearing surface and central site of femoral head in spongy bone also are not significantly different ($P = 0.4064$).

Results from Raman spectroscopy indicate that Raman parameters can distinguish OA bone tissue from normal bone tissue. We verify that the content of organic and mineral components significantly changes in subchondral bone in human OA. The subchondral bone from OA patients in comparison with control subject is less mineralized, due to a decrease in the hydroxyapatite content. However, the extent of carbonate accumulation in the apatite crystal lattice increases, most likely due to deficient mineralization. The alpha helix to random coil band area ratio reveals that collagen matrix in subchondral bone is less ordered in OA disease. We observe that hydroxyapatite to collagen, carbonate apatite to hydroxyapatite and alpha helix to random coil band area ratios are not significantly changed in the differently loaded sites of femoral head. These results show that increased load may not cause the changes in composition and structure of subchondral bone. We confirm that content of mineral and organic components are not significantly different in spongy bone beneath the subchondral bone in OA disease.

4 Conclusion

Raman microspectroscopy was used to identify the biochemical changes in subchondral and underlying spongy bone of femoral heads collected from patients diagnosed with degenerative disease of the hip joint. We demonstrated that this spectroscopic method provides detailed chemical information on the extracellular matrix components of bone tissue and allows us to determine the disorder in collagen's secondary structure. Parameters such as hydroxyapatite to collagen ratio, carbonate apatite to hydroxyapatite ratio and alpha helix to random coil ratio

indicate alternations in composition and structure in subchondral bone of OA patients. On the other hand, significant changes are not visible in composition and structure of spongy bone beneath the subchondral bone in OA disease. Compositional and structural parameters also are not significantly changed in the differently loaded sites of femoral head. The published results show high potential in distinguishing normal and OA tissue and demonstrate the utility and sensitivity of the Raman microspectroscopy method for the study of OA disease. Determining the properties of subchondral and spongy bone permits better understanding of OA disease progression and can help find the origins of this disease. In future studies, data from other analytical methods, such as FTIR spectroscopy can be used to confirm results obtained by Raman spectroscopy. Our investigation contributes to development of a method in identification of human OA. Fiberoptic technology is frequently used through the arthroscopes to evaluate joints in the clinical setting. Raman instruments are compatible with fiberoptic probes and could be used directly in arthroscopic surgery. Esmonde-White et al. showed the use of Raman spectroscopy for arthroscopy of human joint tissues using a custom-built fiber-optic probe[36] The ability to utilize Raman spectroscopy to obtain properties of OA bone through arthroscopes make this an exceedingly powerful technique.

Acknowledgments

The samples were prepared at the Medical University in Poznan. All the measurements were carried out on Renishaw inVia microscope at the Poznan University of Technology. All experimental procedures were approved by the local bioethical commission at the Wielkopolska Medical Chamber in Poznan (No 843/09). The author Tomasz Buchwald declares that he is a scholarship holder within the project "Scholarship support for PH.D. students specializing in majors strategic for Wielkopolska's development," Sub-measure 8.2.2 Human Capital Operational Programme, co-financed by European Union under the European Social Fund.

References

1. D. S. Howell, A. I. Sapolsky, and J. C. Pita, "The pathogenesis of degenerative joint disease," in *Current Concepts*, pp. 5–28, Scope Publication, New York (1982).
2. K. Chiba et al., "In vivo structural analysis of subchondral trabecular bone in osteoarthritis of the hip using multi-detector row CT," *Osteoarthr. Cartil.* **19**(2), 180–185 (2011).
3. F. T. Hoaglund and L. S. Steinbach, "Primary osteoarthritis of the hip: etiology and epidemiology," *J. Am. Acad. Orthop. Surg.* **9**(5), 320–327 (2001).
4. P. A. Dieppe and L. S. Lohmander, "Pathogenesis and management of pain in osteoarthritis," *Lancet* **365**(9463), 965–973 (2005).
5. R. Ganz et al., "The etiology of osteoarthritis of the hip: an integrated mechanical concept," *Clin. Orthop. Relat. Res.* **466**(2), 264–272 (2008).
6. D. T. Felson et al., "Osteoarthritis: new insights. Part 1: the disease and its risk factors," *Ann. Int. Med.* **133**(8), 635–646 (2000).
7. D. T. Felson and T. Neogi, "Osteoarthritis: is it a disease of cartilage or of bone?," *Arthritis Rheum.* **50**(2), 341–344 (2004).
8. T. R. Oegema et al., "The interaction of the zone of calcified cartilage and subchondral bone in osteoarthritis," *Microsc. Res. Tech.* **37**(4), 324–332 (1997).
9. D. B. Burr and M. B. Schaffler, "The involvement of subchondral mineralized tissues in osteoarthrosis: Quantitative microscopic evidence," *Microsc. Res. Tech.* **37**(4), 343–357 (1997).
10. E. L. Radin et al., "The role of bone changes in the degeneration of articular cartilage in osteoarthritis," *Acta Orthop. Belg.* **44**(1), 55–63 (1978).
11. E. L. Radin, I. L. Paul, and R. M. Rose, "Role of mechanical factors in pathogenesis of primary osteoarthritis," *Lancet* **299**(7749), 519–522 (1972).
12. D. B. Burr, "The importance of subchondral bone in the progression of osteoarthritis," *J. Rheumatol. Suppl.* **70**, 77–80 (2004).
13. A. J. Bailey et al., "Biochemical and mechanical properties of subchondral bone in osteoarthritis," *Biorheology* **41**(3–4), 349–358 (2004).
14. J. S. Day et al., "Adaptation of subchondral bone in osteoarthritis," *Biorheology* **41**(3–4), 359–368 (2004).
15. B. Li et al., "The electron microscope appearance of the subchondral bone plate in the human femoral head in osteoarthritis and osteoporosis," *J. Anat.* **195**(1), 101–110 (1999).
16. B. Li and R. M. Aspden, "Composition and mechanical properties of cancellous bone from the femoral head of patients with osteoporosis or osteoarthritis," *J. Bone Miner. Res.* **12**(4), 641–651 (1997).
17. M. D. Grynpas et al., "Subchondral bone in osteoarthritis," *Calcif. Tissue Int.* **49**(1), 20–26 (1991).
18. V. L. Ferguson, A. J. Bushby, and A. Boyde, "Nanomechanical properties and mineral concentration in articular calcified cartilage and subchondral bone," *J. Anat.* **203**(2), 191–202 (2003).
19. L. Diaz-Flores et al., "Pericytes as a supplementary source of osteoblasts in periosteal osteogenesis," *Clin. Orthop. Relat. Res.* **275**, 280–286 (1992).
20. S. Harada and G. A. Rodan, "Control of osteoblast function and regulation of bone mass," *Nature* **423**(6937), 349–355 (2003).
21. J. A. Buckwalter et al., "Bone biology part I: structure, blood supply, cells, matrix, and mineralization," *J. Bone Joint Surg.* **77**(8), 1256–1275 (1995).
22. J. A. Buckwalter et al., "Bone biology part II: formation, form, modeling, remodeling, and regulation of cell function," *J. Bone Joint Surg.* **77**(8), 1276–1289 (1995).
23. J. Sierpowska et al., "Effect of human trabecular bone composition on its electrical properties," *Med. Eng. Phys.* **29**(8), 845–852 (2007).
24. R. Garrett and C. M. Grisham, *Biochemistry*, 4th ed., Brooks/Cole, Cengage Learning, Boston, pp. 134–180 (2010).
25. B. Brodsky et al., "Triple-helical peptides: an approach to collagen conformation, stability, and self-association," *Biopolymers* **89**(5), 345–353 (2008).
26. P. V. Hauschka and W. F. Harrington, "Collagen structure in solution. IV. Conformational properties of refolded cross-linked chains," *Biochemistry* **9**(19), 3745–3754 (1970).
27. M. D. Morris and P. Matousek, *Emerging Raman Applications and Techniques in Biomedical and Pharmaceutical Fields, Biological and Medical Physics, Biomedical Engineering*, Springer Heidelberg, Dordrecht, London, New York, pp. 347–364 (2010).
28. H. Isaksson et al., "Infrared spectroscopy indicates altered bone turnover and remodeling activity in renal osteodystrophy," *J. Bone Miner. Res.* **25**(6), 1360–1366 (2010).
29. R. Servaty et al., "Hydration of polymeric components of cartilage—an infrared spectroscopic study on hyaluronic acid and chondroitin sulfate," *Int. J. Biol. Macromol.* **28**(2), 121–127 (2001).
30. N. S. Lim et al., "Early detection of biomolecular changes in disrupted porcine cartilage using polarized Raman spectroscopy," *J. Biomed. Opt.* **16**(1), 017003 (2011).
31. M. D. Morris and G. S. Mandair, "Raman assessment of bone quality," *Clin. Orthop. Relat. Res.* **469**(8), 2160–2169 (2010).
32. A. Boskey and N. P. Camacho, "FT-IR imaging of native and tissue-engineered bone and cartilage," *Biomaterials* **28**(15), 2465–2478 (2007).
33. G. Penel et al., "Composition of bone and apatitic biomaterials as revealed by intravital Raman microspectroscopy," *Bone* **36**(5), 893–901 (2005).
34. M. Kozielski et al., "Determination of composition and structure of spongy bone tissue in human head of femur by Raman spectral mapping," *J. Mater. Sci.: Mater. Med.* **22**(7), 1653–1661 (2011).
35. H.-U. Gramlich and B. Yan, *Infrared and Raman Spectroscopy of Biological Materials*, Marcel Decker, New York (2001).
36. K. A. Esmonde-White et al., "Fiber-optic Raman spectroscopy of joint tissues," *Analyst* **136**(8), 1675–1685 (2011).

37. M. Sato et al., "Hydroxyapatite maturity in the calcified cartilage and underlying subchondral bone of guinea pigs with spontaneous osteoarthritis: analysis by Fourier Transform infrared microspectroscopy," *Acta Histochem. Cytochem.* **37**(2), 101–107 (2004).
38. K. A. Dehring, B. J. Roessler, and M. D. Morris, "Correlating chemical changes in subchondral bone mineral due to aging or defective type II collagen by Raman spectroscopy," *Proc. SPIE* **6430**, 64301B (2007).
39. L. M. Miller et al., "Alterations in mineral composition observed in osteoarthritic joints of cynomolgus monkeys," *Bone* **35**(2), 498–506 (2004).
40. K. A. Dehring et al., "Correlating changes in collagen secondary structure with aging and defective type II collagen by Raman spectroscopy," *Appl. Spectrosc.* **60**(4), 366–372 (2006).
41. K. A. Dehring et al., "Identifying chemical changes in subchondral bone taken from murine knee joints using Raman spectroscopy," *Appl. Spectrosc.* **60**(10), 1134–1141 (2006).
42. A. M. Croxford et al., "Chemical changes demonstrated in cartilage by synchrotron infrared microspectroscopy in an antibody-induced murine model of rheumatoid arthritis," *J. Biomed. Opt.* **16**(6), 066004 (2011).
43. K. A. Esmonde-White et al., "Raman spectroscopy of synovial fluid as a tool for diagnosing osteoarthritis," *J. Biomed. Opt.* **14**(3), 034013 (2009).
44. E. David-Vaudey et al., "Fourier Transform infrared imaging of focal lesions in human osteoarthritic cartilage," *Eur. Cells Mater.* **22**(10), 51–60 (2005).
45. K. A. Dooley et al., "Stress mapping of undamaged, strained, and failed regions of bone using Raman spectroscopy," *J. Biomed. Opt.* **14**, 044018 (2009).
46. H. C. Batra and J. Charnley, "Existence and incidence of osteoid in osteoarthritis femoral heads," *J. Bone Joint Surg.* **51**(2), 366–371 (1969).
47. J. H. Kellgren and J. S. Lawrence, "Radiological assessment of osteo-arthrosis," *Ann. Rheum. Dis.* **16**(4), 494–502 (1957).
48. J. H. Kellgren and J. S. Lawrence, *Atlas of Standard Radiographs*, Blackwell Scientific Oxford, UK (1963).
49. R Development Core Team, *R: A Language and Environment for Statistical Computing*, R Foundation for Statistical Computing, Vienna, Austria (2009).
50. M. Kazanci et al., "Bone osteonal tissues by Raman spectra mapping: orientation-composition," *J. Struct. Biol.* **156**(3), 489–496 (2006).
51. M. Kazanci et al., "Raman imaging of two orthogonal planes within cortical bone," *Bone* **41**(3), 456–461 (2007).
52. S. R. Goodyear et al., "A comparison of cortical and trabecular bone from C57 Black 6 mice using Raman spectroscopy," *Bone* **44**(5), 899–907 (2009).
53. M. Raghavan et al., "Quantitative polarized Raman spectroscopy in highly turbid bone tissue," *J. Biomed. Opt.* **15**(3), 037001 (2010).
54. C. P. Tarnowski, M. A. Ignelzi, and M. D. Morris, "Mineralization of developing mouse calvaria as revealed by Raman microspectroscopy," *J. Bone Miner. Res.* **17**(6), 1118–1126 (2002).
55. A. Carden et al., "Ultrastructural changes accompanying the mechanical deformation of bone tissue: a Raman imaging study," *Calcif. Tissue Int.* **72**(2), 166–175 (2003).
56. S. Gamsjaeger et al., "Cortical bone composition and orientation as a function of animal and tissue age in mice by Raman spectroscopy," *Bone* **47**(2), 392–399 (2010).
57. J. M. Wallace et al., "Inbred strain-specific effects of exercise in wild type and biglycan deficient mice," *Ann. Biomed. Eng.* **38**(4), 1607–1617 (2010).
58. Z. Chi et al., "UV resonance Raman-selective amide vibrational enhancement: quantitative methodology for determining protein secondary structure," *Biochemistry* **37**(9), 2854–2864 (1998).